Perturbation scheme for a fluxon in a curved Josephson junction

T. Dobrowolski* and A. Jarmoliński
Institute of Physics UP, Podchorążych 2, 30-084 Cracow, Poland
(Received 25 April 2017; published 17 July 2017)

The kink solution in the long Josephson junction is studied. The perturbation scheme of constructing the fluxon solution in curved junction is formulated. The prediction from the perturbation scheme is compared with the prediction that follows from the numerical studies of the complete field model.

DOI: 10.1103/PhysRevE.96.012214

I. INTRODUCTION

For many years the quantum macroscopic systems have attracted the attention of many researchers. The best-known physical systems that (in sufficiently low temperatures) appear in coherent states are quantum liquids He^3 and He^4, atomic Bose-Einsten condensate and superconducting materials. The effective description of these systems is given by the nonlinear solitonic equations [1]. The quantum properties of these systems are used in many technical applications. The leading role in this field is played by superconductors. In particular, superconductors can be arranged in a device (that is, not simply connected system) known as a Josephson junction. Due to the fact that in a superconducting state each electrode is a strongly correlated system, they can be described by the many-particle wave functions. The modulus of such function describes the square root of the density of the Cooper pairs. Because the thickness of the dielectric layer is very small, those two electrodes are not independent quantum systems. The macroscopic wave functions overlap and the phases of the wave functions start to play a nontrivial dynamical role. The main effect, which is connected with overlapping of the wave functions, is tunneling of Cooper pairs from one to the other superconducting electrode. This phenomenon was first predicted by Josephson [2] and then confirmed experimentally by Anderson and Rowell [3]. The leading variable that describes the dynamics of this system is the gauge-invariant phase difference ϕ. The dynamical properties of this variable are described by the sine-Gordon equation [4]. The properties and applications of this model are described in many texts [5]. The properties of the Josephson junction are modified in the curved junctions. The studies of this system were performed in the framework of the geometrical formalism used in many branches of science [6] and the final outcome of these considerations concern constant and position-dependent curvatures as well [7]. In these papers the junction is represented by a curve or a surface with nonzero external curvatures.

In the literature there is also other interesting approach [8] concerning curved two-dimensional junctions. In this approach, the junction is represented by the flat surface (the surface with zero external curvatures) but curvature effects follow from the curvature of the boundaries of this system.

In the present paper we consider the modified sine-Gordon equation that describes the dynamics of the gauge-invariant phase difference in the curved junction with slowly varying curvatures. In the next section we construct a perturbation scheme that provides an approximate description of the fluxon in the curved junction. Section III contains numerical studies of the gauge-invariant phase difference ϕ for the static kink. In this section we use the relaxation method in order to obtain the static kink profile [9]. The same solution is obtained in the framework of the perturbation scheme in Sec. IV. The last section contains remarks.

II. FLUXON IN CURVED JOSEPHSON JUNCTION

The dynamics of the fluxon in case of slowly varying curvature is described by the modified sine-Gordon equation

$$\partial_t^2\phi - \partial_s(\mathcal{F}\partial_s\phi) + \sin\phi = 0, \tag{1}$$

where the function $\mathcal{F}(s)$ contains information about the curvature of the considered space and has the following form:

$$\mathcal{F}(s) = \frac{1}{aK(s)} \ln\left[\frac{2+aK(s)}{2-aK(s)}\right]. \tag{2}$$

Here $K(s)$ is the curvature of the central curve of the junction and a is thickness of the dielectric layer. The curvature-dependent function $\mathcal{F}$ is presented in Fig. 1 as a function of the modulus of the curvature. The physical regime of the variable $|aK(s)|$ is limited to the interval $[0,2)$. This restriction on curvatures follows from the fact that for presumed constant thickness of the dielectric layer, for bigger curvatures, one of the electrodes disappear [9]. In the static case the field Eq. (1) can be written in a simpler form:

$$\partial_s(\mathcal{F}\partial_s\phi) = \sin\phi. \tag{3}$$

This equation, in particular for the case of constant curvature, has a kink solution with the same profile like a kink in flat space but where its width is magnified by the curvature-dependent factor $1/\sqrt{\mathcal{F}}$, i.e.,

$$\phi(s) = 4\arctan e^{\frac{1}{\sqrt{\mathcal{F}}}(s-s_0)}. \tag{4}$$

The first derivative of this function with respect to the space variable represents distribution of the magnetic flux in the junction. This distribution for the flat (gray contour) and curved space (black contour) are compared in Fig. 2. The existence of the kink solutions in the curved case for nonconstant curvatures follows from the Bogomolny argument [9]. In the case of nonconstant curvatures, i.e., for $\mathcal{F} \neq$ const, the solutions can be constructed with the help of perturbation scheme. First, in order to formulate this scheme, we have to identify the perturbation parameter. In a realistic junction we can expect that the thickness of the superconducting electrode is not less than the curvature radius of the junction. On the other hand, in

*Corresponding author: dobrow@up.krakow.pl

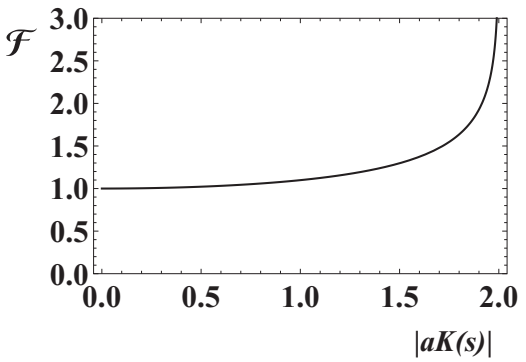

FIG. 1. The curvature-dependent function $\mathcal{F}$ as a function of modulus of dimensionless quantity aK.

such a junction the superconducting electrode is much thicker than the dielectric layer and, therefore, even at positions where the curvature radius is minimal we can expect $R_{\min} \gg a$. In these circumstances we can identify the natural perturbation parameter as follows: $\varepsilon \equiv \frac{a}{R_{\min}}$. Let us notice that the dimensionless quantity $aK(s) = \frac{a}{R(s)} = \frac{a}{R_{\min}} \frac{R_{\min}}{R(s)}$ can be represented as the product of the perturbation parameter and limited function $g(s)$, i.e., $aK(s) = \frac{a}{R_{\min}} g(s) = \varepsilon g(s)$. Next we expand the function $\mathcal{F}$ for small curvatures, i.e., for small $\varepsilon g(s)$,

$$\mathcal{F}(s) = \frac{1}{\varepsilon g(s)} \ln\left[\frac{2+\varepsilon g(s)}{2-\varepsilon g(s)}\right] = \sum_{n=0}^{\infty} \frac{\varepsilon^{2n} g^{2n}}{2^{2n}(2n+1)}$$
$$\approx 1 + \frac{1}{12}\varepsilon^2 g^2 + \frac{1}{80}\varepsilon^4 g^4 + \cdots . \tag{5}$$

Similarly, we can expand gauge-invariant phase difference with respect to perturbational parameter ε,

$$\phi(t,s) = \sum_{n=0}^{\infty} \varepsilon^n \phi_n(s,t)$$
$$= \phi_0(t,s) + \varepsilon\phi_1(t,s) + \varepsilon^2\phi_2(t,s)$$
$$+\varepsilon^3\phi_3(t,s) + \cdots . \tag{6}$$

Additionally, for the sake of convenience, we separate the field ϕ on the zero-order term and perturbational correction ψ, i.e.,

$$\phi = \phi_0 + \psi, \quad \psi = \sum_{n=1}^{\infty} \varepsilon^n \phi_n(s,t). \tag{7}$$

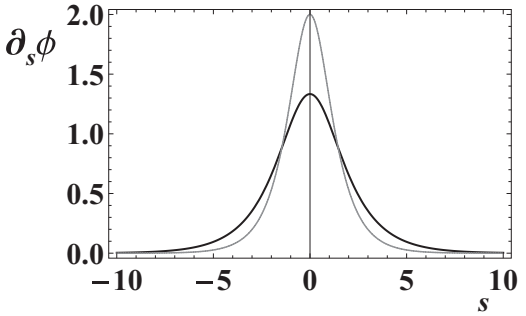

FIG. 2. The first derivative of the field variable ϕ for the kink solution in the flat junction (gray line) and in the curved junction (black line). The curvature in this plot is $aK = 1.95$.

The perturbational scheme of this type was applied in the series of papers connected with the solitonic physics [10,11]. According to this scheme, we separate the equation of motion into different orders of expansion in the perturbational parameter. We put the expansions (5), (6), and (7) into the equation of motion (1) and obtain:

$$\sum_{n=0}^{\infty} \varepsilon^n \partial_t^2 \phi_n - \partial_s \left(\sum_{n=0}^{\infty} \frac{\varepsilon^{2n} g^{2n}}{2^{2n}(2n+1)} \sum_{k=0}^{\infty} \varepsilon^k \partial_s \phi_k \right)$$
$$+ \sin(\phi_0 + \psi) = 0. \tag{8}$$

Next, we rearrange the second term in Eq. (8),

$$\sum_{n=0}^{\infty} \varepsilon^n \partial_t^2 \phi_n - \sum_{n=0}^{\infty} \varepsilon^n \sum_{m=0}^{n} \frac{1}{2^{2m}(2m+1)} \varepsilon^m \, \partial_s (g^{2m} \partial_s \phi_{n-m})$$
$$+ \sin(\phi_0 + \psi) = 0. \tag{9}$$

From this expansion we extract the second space derivatives of the subsequent orders of the gauge-invariant phase difference:

$$\sum_{n=0}^{\infty} \varepsilon^n \left(\partial_t^2 \phi_n - \partial_s^2 \phi_n\right)$$
$$- \sum_{n=1}^{\infty} \varepsilon^n \sum_{m=1}^{n} \frac{1}{2^{2m}(2m+1)} \varepsilon^m \, \partial_s (g^{2m} \partial_s \phi_{n-m})$$
$$+ \sin(\phi_0 + \psi) = 0. \tag{10}$$

We expand the sine around the zero-order component of the field ϕ,

$$\sin(\phi_0 + \psi) = \sin\phi_0 \sum_{n=0}^{\infty} \frac{(-1)^n}{(2n)!} \psi^{2n}$$
$$+ \cos\phi_0 \sum_{n=0}^{\infty} \frac{(-1)^n}{(2n+1)!} \psi^{2n+1}, \tag{11}$$

where the nth power of the auxiliary field ψ can be expressed as a function of the appropriate products of the components of the field ϕ,

$$\psi^n = \sum_{k_n=n}^{\infty} \varepsilon^{k_n} \sum_{k_{n-1}=n-1}^{k_n-1} \sum_{k_{n-2}=n-2}^{k_{n-1}-1}$$
$$\cdots \sum_{k_2=2}^{k_3-1} \sum_{k_1=1}^{k_2-1} \phi_{k_n-k_{n-1}} \phi_{k_{n-1}-k_{n-2}} \cdots \phi_{k_2-k_1} \phi_{k_1}. \tag{12}$$

In Eq. (11), we extract the sine term and the cosine terms in all orders of expansion starting from the first order,

$$\sin(\phi_0 + \psi) = \sin\phi_0 + \sin\phi_0 \sum_{n=1}^{\infty} \frac{(-1)^n}{(2n)!} \psi^{2n}$$
$$+ \cos\phi_0 \sum_{n=1}^{\infty} \varepsilon^n \phi_n$$
$$+ \cos\phi_0 \sum_{n=1}^{\infty} \frac{(-1)^n}{(2n+1)!} \psi^{2n+1}. \tag{13}$$

If we take into account the last formula, then Eq. (10) can be transformed to the form

$$\begin{aligned}&\left(\partial_t^2\phi_0-\partial_s^2\phi_0+\sin\phi_0\right)+\sum_{n=1}^{\infty}\varepsilon^n\hat{\mathcal{L}}\phi_n\\&=\sin\phi_0\sum_{n=1}^{\infty}\frac{(-1)^{n+1}}{(2n)!}\psi^{2n}\\&+\cos\phi_0\sum_{n=1}^{\infty}\frac{(-1)^{n+1}}{(2n+1)!}\psi^{2n+1}\\&+\sum_{n=1}^{\infty}\varepsilon^n\sum_{m=1}^{n}\frac{1}{2^{2m}(2m+1)}\,\varepsilon^m\,\partial_s(g^{2m}\partial_s\phi_{n-m}),\end{aligned}\tag{14}$$

where $\widehat{\mathcal{L}}$ is the following linear operator:

$$\widehat{\mathcal{L}}\equiv\partial_t^2-\partial_s^2+\cos\phi_K.\tag{15}$$

From Eq. (14), we extract the zero-order term of expansion of the field equation:

$$\partial_t^2\phi_0-\partial_s^2\phi_0+\sin\phi_0=0.\tag{16}$$

This equation coincides with the sine-Gordon equation in the flat space. The zero-order equation provides the solution that is a base for further perturbation. In our case, we choose the stationary kink (with unit topological charge). This choice allows us to determine the influence of the curvature on the kink motion and, moreover, the kink profile. In the lowest order of expansion, we have the stationary kink solution which satisfies the only nonlinear equation in the whole scheme, i.e., the zero-order equation

$$\phi_0(t,s)=\phi_K(s-vt)=4\arctan[e^{\gamma(s-s_0-vt)}],\tag{17}$$

where $\gamma=\frac{1}{\sqrt{1-v^2}}$ and v is the kink speed. If we take into account the zero order (16), then Eq. (14) simplifies as follows:

$$\begin{aligned}&\sum_{n=1}^{\infty}\varepsilon^n\hat{\mathcal{L}}\phi_n\\&=\sin\phi_0\sum_{n=1}^{\infty}\frac{(-1)^{n+1}}{(2n)!}\psi^{2n}+\cos\phi_0\sum_{n=1}^{\infty}\frac{(-1)^{n+1}}{(2n+1)!}\psi^{2n+1}\\&+\sum_{n=1}^{\infty}\varepsilon^n\sum_{m=1}^{n}\frac{1}{2^{2m}(2m+1)}\,\varepsilon^m\,\partial_s(g^{2m}\partial_s\phi_{n-m}).\end{aligned}\tag{18}$$

Next, we enumerate the last term in the above formula,

$$\begin{aligned}&\sum_{n=1}^{\infty}\varepsilon^n\hat{\mathcal{L}}\phi_n\\&=\sin\phi_0\sum_{n=1}^{\infty}\frac{(-1)^{n+1}}{(2n)!}\psi^{2n}+\cos\phi_0\sum_{n=1}^{\infty}\frac{(-1)^{n+1}}{(2n+1)!}\psi^{2n+1}\\&+\sum_{n=1}^{\infty}\sum_{m=n+1}^{2n}\varepsilon^m\frac{1}{2^{2(m-n)}[2(m-n)+1]}\\&\times\partial_s[g^{2(m-n)}\partial_s\phi_{2n-m}].\end{aligned}\tag{19}$$

If we use the formula (12) then we can extract the subsequent orders of expansion in Eq. (19). As a result, we obtain the infinite number of equations for the functions ϕ_n. For example, in the first order of expansion ($n=1$) we obtain the following equation:

$$\widehat{\mathcal{L}}\phi_1(t,s)=0.\tag{20}$$

All equations obtained in higher orders of expansion ($n>1$) are also defined by the same linear operator,

$$\widehat{\mathcal{L}}\phi_n(t,s)=f_n(\phi_0,\phi_1,\ldots,\phi_{n-1}).\tag{21}$$

Let us notice that all obtained equations are nonhomogenous but linear because the functions f_n do not depend on ϕ_n. If we put the solutions of the equations of lowest orders $\{\phi_0,\phi_1,\ldots,\phi_{n-1}\}$ into f_n, then this function becomes some explicit function of t and s variables. For example, in the first orders of expansion these functions have the form

$$f_1=0,\qquad f_2=\tfrac{1}{2}(\sin\phi_0)\,\phi_1^2+\tfrac{1}{12}\,\partial_s(g^2\partial_s\phi_0),\tag{22}$$

$$f_3=(\sin\phi_0)\,\phi_1\phi_2+\tfrac{1}{6}(\cos\phi_0)\,\phi_1^3+\tfrac{1}{12}\,\partial_s(g^2\partial_s\phi_1),\tag{23}$$

and

$$\begin{aligned}f_4=&(\sin\phi_0)\left(\phi_1\phi_3-\tfrac{1}{24}\,\phi_1^4+\tfrac{1}{2}\,\phi_2^2\right)\\&+\tfrac{1}{2}(\cos\phi_0)\phi_1^2\phi_2+\tfrac{1}{12}\,\partial_s(g^2\partial_s\phi_2)+\tfrac{1}{80}\,\partial_s(g^4\partial_s\phi_0).\end{aligned}\tag{24}$$

This perturbation scheme is well formulated in the sense that if we know the Green function for the operator $\widehat{\mathcal{L}}$, then the subsequent corrections can be found by integration of the functions f_n with this Green function. The Green function for the operator $\widehat{\mathcal{L}}$ has been studied in several papers connected with nonlinear Klein-Gordon equations [12]. For the completeness of the presentation we recall the main results. At the beginning, let us notice that for the stationary kink (17) the last term defining the operator can be transformed as follows:

$$\cos\phi_K=1-2\mathrm{sech}^2(s-s_0-vt).$$

In all orders of expansion, we have to solve the differential equation of the form

$$\widehat{\mathcal{L}}\phi=\partial_t^2\phi-\partial_s^2\phi+[\cos\phi_K(s-vt)]\phi=f(t,s).\tag{25}$$

This equation simplifies in the comoving coordinates which, in the case of stationary kink, are related with the original coordinates by the Lorentz boost

$$\bar{t}=\gamma[t-v(s-s_0)],\ \bar{s}=\gamma(s-s_0-vt).$$

The linear operator in new coordinates has a simplified potential,

$$\widehat{\mathcal{L}}\phi=\partial_{\bar{t}}^2\phi-\partial_{\bar{s}}^2\phi+[\cos\phi_K(\bar{s})]\phi=f(\bar{t},\bar{s}).\tag{26}$$

The Green function for this operator is defined by the equation

$$\widehat{\mathcal{L}}G=\delta(\bar{t}-\bar{t}')\delta(\bar{s}-\bar{s}').\tag{27}$$

A particular solution of initial value problem defined by Eq. (26) and initial conditions imposed on ϕ and its first time derivative at $t=0$ can be found from the formula

$$\phi(\bar{t},\bar{s})=\int_0^{\infty}d\bar{t}'\int_{-\infty}^{+\infty}d\bar{s}'G(\bar{t},\bar{s};\bar{t}',\bar{s}')f(\bar{t}',\bar{s}'),\tag{28}$$

where the Green function has the explicit form

$$G(\bar{t},\bar{s};\bar{t}',\bar{s}') = \frac{1}{8\pi i\gamma^2}(\bar{t}-\bar{t}')\theta(\bar{t}-\bar{t}')\mathrm{sech}\bar{s}\,\mathrm{sech}\bar{s}'\int_{-\infty}^{+\infty} dk e^{ik(\bar{s}-\bar{s}')} \times\left\{\frac{[\tanh\bar{s}-i\gamma(k+v\omega)][\tanh\bar{s}'+i\gamma(k+v\omega)]}{\omega(vk+\omega)^2}e^{i\omega(t-t')}\right. - \left.\frac{[\tanh\bar{s}-i\gamma(k-v\omega)][(\tanh\bar{s}'+i\gamma(k-v\omega)]}{\omega(vk-\omega)^2}e^{-i\omega(t-t')}\right\}, \tag{29}$$

where ω and k are related by the dispersion relation $\omega = \sqrt{1+k^2}$.

III. STATIC KINK ON CURVED BACKGROUND—NUMERICAL SOLUTION

In this section we will obtain the static kink on a curved background. First, we fix the position-dependent curvature. We know that the curvature of the junction corresponds to the existence of some effective potential that affects the kink motion [13,14]. The kink can be static only in the local minimum of this potential. Moreover, we can always choose the system of coordinates in a way where this minimum coincides with the origin of the system of coordinates. We consider the following example of the position-dependent curvature:

$$aK(s) = \frac{A}{1+5(s-1)^2} + \frac{A}{1+5(s+1)^2}. \tag{30}$$

Due to symmetry of this function with respect to the origin of the coordinate system, the natural candidate for the rest position of the static kink is $s_0 = 0$. During the numerical studies we use the field equation equipped in the dissipation term

$$\partial_t^2\phi + \gamma\partial_t\phi - \partial_s(\mathcal{F}\partial_s\phi) + \sin\phi = 0. \tag{31}$$

According to the relaxation method, we choose the initial condition that is sufficiently close to the expected final configuration. In our case, this initial configuration has a form of the static kink, characteristic for flat space, located in the origin of the coordinate system. The presence of the dissipation term is responsible for removing some part of the energy from the system and tendency of the field to reach the configuration with minimal energy. This is a reason why the static sector of the model (31) is identical with the static sector of the model (1). We applied the implicit backward differentiation formulas (BDF) procedure with the maximum size of a single step limited to 0.1. The effective accuracy is fixed at the level of three digits. In order to emphasize the difference between the kink profile in the flat and curved junctions we consider the first space derivative of the gauge-invariant phase difference. Moreover, this quantity represents distribution of the magnetic flux in the junction. In the numerics the amplitude of the curvature is chosen as follows: $A = 1.9$. Additionally, we choose the dissipation constant $\gamma = 5$. This value guarantees both quick dissipation of the energy from the system and sufficiently quick evolution of the field configuration. The final configuration in these conditions became stable before $t = 10$. The shape of the final configuration (its first space derivative) in Fig. 3 is represented by black continuous line. The dashed gray line represents the curvature of the junction. The static kink configuration in this case is located in the origin of the coordinate system.

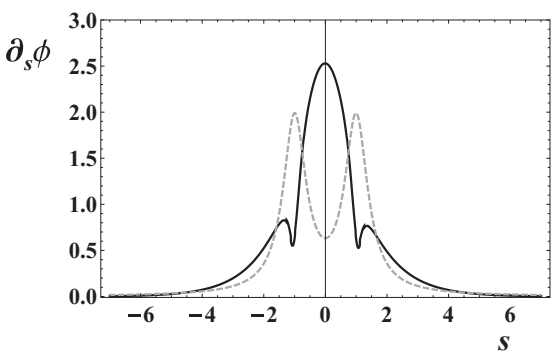

FIG. 3. The static kink in the curved junction. The dashed gray line represents the curvature of the junction and the black continuous line represents the space gradient of the gauge-invariant phase difference. The configuration was stabilized before the instant $t = 10$ and no change was observed until $t = 100$. The parameters chosen in this plot are the following $A = 1.9$, $\gamma = 5$.

IV. STATIC KINK ON CURVED BACKGROUND—APPROXIMATE SOLUTIONS

In case of static solutions the perturbational scheme is defined by the equations of the form

$$\widehat{\mathcal{L}}\phi_n = -\partial_s^2\phi_n + \cos\phi_K(s)\phi_n = f_n(t,s). \tag{32}$$

The solutions of this equation and the Green function were presented in a number of papers [10,15]. Here we use these results. The effects of curvature in perturbational scheme first appear in the second order because in the first order we have $f_1 = 0$ and therefore we approximate the solution by the expansion

$$\phi \approx \phi_0 + \varepsilon\phi_1 + \varepsilon^2\phi_2. \tag{33}$$

Let us recall that the ϕ_0 is kink solution in a flat space and one of solutions ϕ_1 of the equation (32) represents translational mode. Because we are interested in the static kink, we choose the trivial solution $\phi_1 = 0$. The second function f_2 in this case simplifies to the term that solely depends on the curvature, i.e., $f_2 = \frac{1}{12}\partial_s(g^2\partial_s\phi_0)$. Let us also notice that the choice $\phi_1 = 0$ makes $f_3 = 0$ and we obtain $\widehat{\mathcal{L}}\phi_3 = 0$, see Eqs. (21) and (23). This observation suggests that the proposed approximation extends up to the third order. Due to clarity of presentation and the physical meaning of the space derivative of the gauge-invariant phase difference we consider expansion of

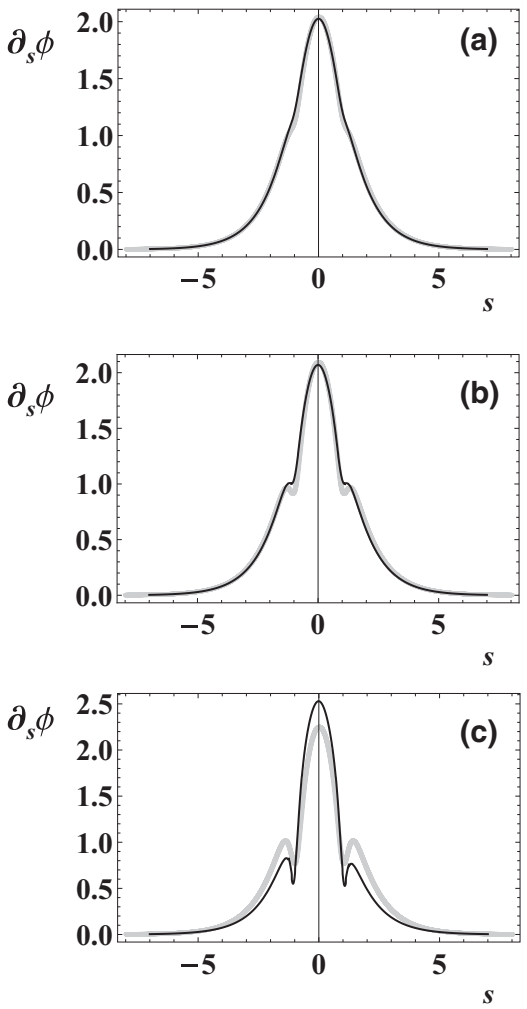

FIG. 4. The space gradient of the gauge-invariant phase difference calculated from the perturbational scheme (gray line) and the numerical solution obtained in the model (31) (black line). The figures (a) $A = 1$, (b) $A = 1.5$, and (c) $A = 1.9$ correspond to different values of the curvature parameter A.

the gradient of the field ϕ,

$$\partial_s\phi \approx \partial_s\phi_0 + \varepsilon^2\partial_s\phi_2. \tag{34}$$

In Fig. 4, we perform comparison of the perturbational scheme for three different values of the parameter A (i.e., for $A = 1$, $A = 1.5$, and $A = 1.9$) with the numerical results for the same values of this parameter. The results of the perturbational scheme are represented by the gray line. On the other hand, in all figures the numerical results are represented by continuous black line.

V. REMARKS

We formulated the complete perturbation scheme that allows for description of the evolution of the kink in the curved Josephson junction. The method relies on the infinite number of equations. The first of the equations is the only nonlinear equation in the scheme. The solution of this equation is some field configuration being a solution in the flat space. This configuration is modified due to curvature effects. The other equations in the scheme are linear equations defined by the same linear operator $\widehat{\mathcal{L}}$. The Green function for this operator is known in the explicit form. This knowledge makes the scheme complete. In particular, this method provides possibility to calculate the profiles of the static kinks. On the other hand, in order to obtain the static kink profiles in the curved junction, we used the relaxation method. The numerical profiles obtained in this way were compared with the profiles obtained in the framework of the perturbation scheme. The results obtained in the second-order approximation are compared with the numerical results based on the complete field equation in curved space. This comparison shows good agreement especially for small curvatures.

One of the most promising areas of application for the Josephson device is rapid single flux quantum (RSFQ) electronics [16]. The digital information in these devices is carried by magnetic flux quanta identified with the kink solution of the sine-Gordon model. A particular role in this area can be played by the curved Josephson junctions. On the base of the modified sine-Gordon equation, several geometries were identified which can be used in RSFQ electronic elements. The first interesting shape is responsible for acceleration or deacceleration of fluxons. This element can work in RSFQ circuits as boosters [17]. The other geometry enables separation of fast from slow fluxons. This element can work as a discriminating element in RSFQ electronic devices. Finally, the last identified shape may be used in storing binary data in the form of fluxons [9,18].

ACKNOWLEDGMENT

This work was supported in part by NCN Grant No. 2011/03/B/ST3/00448.

APPENDIX A: RELATION BETWEEN CURVATURE AND THE SHAPE OF THE JUNCTION

As in the main text, we consider curves that are free of torsion. In this case the curve is located in a single plane. Moreover, in order to simplify description, we identify the parameter s with the x variable. The vector field in this case has the form

$$\vec{X}(x) = x\vec{e}_x + f(x)\vec{e}_x.$$

The normal vector to the curve

$$\vec{n} = n_x(x)\vec{e}_x + n_y(x)\vec{e}_y$$

is fixed by the orthogonality and normalization conditions

$$\vec{n}\cdot\vec{X}'(x) = 0, \quad \vec{n}^2 = 1,$$

where $\vec{X}'(x) = \partial_x\vec{X}$ is vector tangent to the curve. The components of the normal vector are as follows:

$$n_x = -\frac{f'(x)}{\sqrt{1+f'(x)^2}}, \quad n_y = \frac{1}{\sqrt{1+f'(x)^2}}.$$

Finally, the curvature of the considered curve is a simple function of the derivatives of the function $f(x)$,

$$K(x) = \vec{n}\cdot\vec{X}'' = \frac{f''(x)}{\sqrt{1+f'(x)^2}}.$$

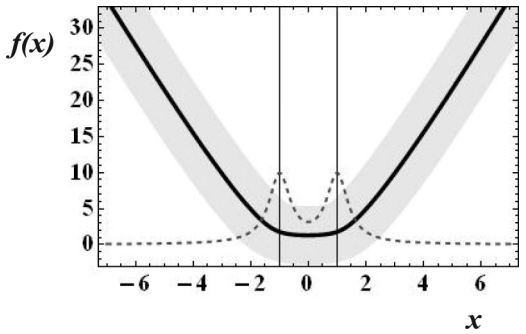

FIG. 5. The shape of the junction that corresponds to the curvature (30). The dashed line represents the curvature. The gray region represents the dielectric layer.

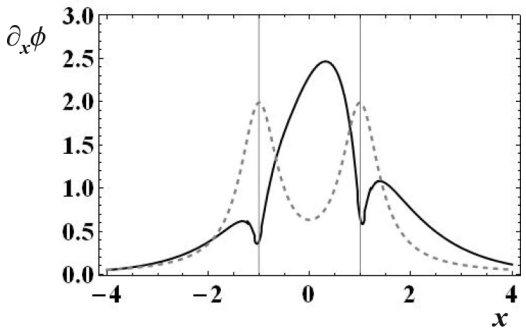

FIG. 6. The final shape of the gradient of the gauge-invariant phase difference ϕ at $t = 1000$. The dashed line represents the curvature of the junction.

Let us notice that the last formula can be used in order to calculate the shape function $f(x)$ whenever we know the explicit form of the curvature $K = K(x)$, i.e.,

$$f''(x) - K(x)\sqrt{1 + f'(x)^2} = 0.$$

In particular, for considered in this paper curvature (30) the shape of the junction, i.e., function $f(x)$ is presented in Fig. 5. For better visualization, we placed the dashed contour that represents the curvature. The thickness of the dielectric layer of the junction is represented by the gray strip.

APPENDIX B: IMPACT OF THE EXTERNAL BIASED CURRENT ON THE CONFINED FLUXON

The other issue is the problem of the stability of the multipeak structure demonstrated, for example, in Fig. 3. The effective dynamics of the fluxon in the curved junction was studied in Ref. [14], where it was shown that the curvature of the junction corresponds to the effective potential experienced by the fluxon. According to the conclusions of this paper, the two curvature peaks form the effective potential barrier that confines the fluxon and deforms its profile. In the present section we check whether this observation remains true if the system is subject to an external biased current flow. We will study the system described by the following equation:

$$\partial_t^2\phi + \gamma\,\partial_t\phi - \partial_x(\mathcal{F}\partial_x\phi) + \sin\phi = J.$$

First, we checked the relaxation time, i.e., the time needed to relax from initial configuration having the form of the free kink configuration (gray line in Fig. 2) to the configuration deformed by the presence of the curvatures in the system (black line in Fig. 3). According to performed simulations, in the case of $\gamma = 1$ and $J = 0$, the final configuration is reached at $t = 8 \equiv \tau$. We use this result as the relaxation time of the considered system for $\gamma = 1$. Here, we lowered the value of the dissipation parameter (in comparison to the previous simulations) in order to increase mobility of the kink. As a result of the performed studies, we observed that the time scale of the kink motion is much longer than the relaxation time in the system and therefore the behavior of the fluxon in the presence of the external current shall be approximated by the method applied in the previous sections. Having the knowledge of the relaxation time τ, we performed simulations for several values of the J parameter. Here we assumed that the normalized current density J is constant. In all numerical experiments we presumed the curvature in the form of (30) and, moreover, $A = 1.9$. The calculations confirmed that there are two regimes of the $|\ J\ |$ parameter. In the first regime the kink is confined between curved regions of the junction (see Fig. 6). The configuration presented in this figure corresponds to $|\ J\ | = 0.2$. In agreement with our expectations the kink structure was stabilized just after the relaxation time τ. The shape of this configuration is slight deformation of the configuration presented in Fig. 3. Next we observed that the deformed kink preserves its form without any changes. Figure 6 presents the kink profile at $t = 1000$.

In the second regime, the kink escapes from the region located between two curvatures and therefore does not form the static structure. In this regime we can expect that the relaxation method provides merely qualitative behavior of the system. The kink in this case is pushed out from the confining region

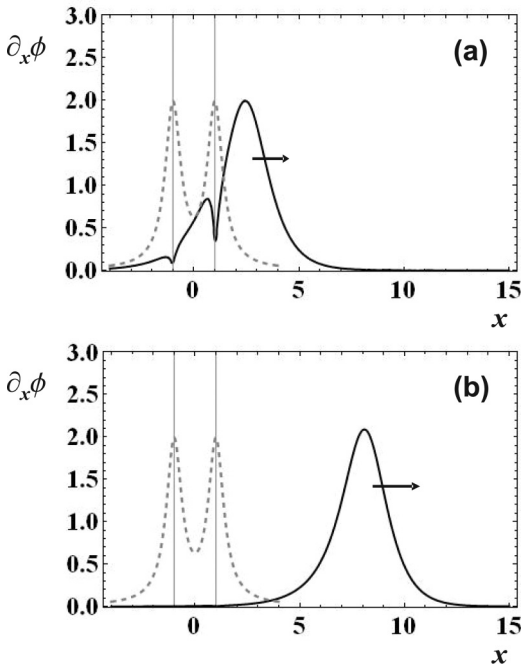

FIG. 7. The evolution of the fluxon. (a) The fluxon leaves the potential hole at $t = 10$. (b) Outside the curved region of the junction the fluxon became free $t = 25$.

of the junction. Figures 7(a) and 7(b) show the evolution of the gradient of the order parameter ϕ for instants exceeding the relaxation time. The value of the external biased current in these plots is $| J | = 0.5$. Figure 7(a) shows the configuration at $t = 10$. One can see that magnetic flux of the fluxon is pushed out from the curved region of the junction. In Figure 7(b) the profile is typical for the free kink. This configuration represents the fluxon at instant $t = 25$.

More accurate studies of this subject will be continued in future work.

[1] A. R. Bishop and T. Schneider, *Solitons and Condensed Matter Physics* (Springer-Verlag, Berlin, 1981); A. S. Davydov, *Solitons in Molecular Systems* (Reidel, Dordrecht, the Netherlands, 1985); A. Barone and G. Paterno, *Physics and Applications of the Josephson Effect* (Wiley, New York, 1982); B. D. Josephson, Adv. Phys. **14**, 419 (1965); A. Barone, F. Esposito, C. J. Magee, and A. C. Scott, Riv. Nuovo Cim. **1**, 227 (1971); J. D. Gibbon, I. N. James, and I. M. Moroz, Phys. Script. **20**, 402 (1979).

[2] B. D. Josephson, Phys. Lett. **1**, 251 (1962).

[3] P. W. Anderson and J. M. Rowell, Phys. Rev. Lett. **10**, 230 (1963).

[4] J. Swihart, J. Appl. Phys. **32**, 461 (1961).

[5] M. J. Ablowitz and P. A. Clarkson, *Solitons, Nonlinear Evolution Equations and Inverse Scattering* (Cambridge University Press, Cambridge, 1999); N. F. Pederson, Solitons in josephson transmission lines, in *Solitons*, edited by S. E. Trullinger *et al.* (Elsevier, Amsterdam, 1986); L. A. Ferreira, B. Piette, and W. J. Zakrzewski, Phys. Rev. E **77**, 036613 (2008); J. Phys. C **128**, 012027 (2008); V. G. Ivancevic and T. T. Ivancevic, J. Geom. Symmetry Phys. **31**, 1 (2013); S. V. Kuplevakhsky and A. M. Glukhov, Phys. Rev. B **73**, 024513 (2006); **76**, 174515 (2007); M. Toda, Ann. Global Anal. Geom. **27**, 257 (2005).

[6] H. Arodź, Nucl. Phys. B **509**, 273 (1998); T. Dobrowolski, Ann. Phys. (NY) **324**, 2473 (2009); J. Geom. Symmetry Phys. **22**, 1 (2011); J. J. Sławianowski, V. Kovalchuk, B. Gołubowska, A. Martens, and E. E. Rożko, Acta Phys. Pol. B **41**, 165 (2010); P. I. Marinov and I. M. Mladenov, J. Geom. Symmetry Phys. **27**, 93 (2012); N. Ogawa, Phys. Rev. E **81**, 061113 (2010).

[7] T. Dobrowolski, Ann. Phys. (N. Y.) **327**, 1336 (2012); A. Jarmoliński and T. Dobrowolski, Physica B: Condens Matter **514**, 24 (2017); T. Dobrowolski, J. Geom. Symmetry Phys. **34**, 13 (2014).

[8] C. Gorria, Yu. B. Gaididei, M. P. Soerensen, P. L. Christiansen, and J. G. Caputo, Phys. Rev. B **69**, 134506 (2004).

[9] T. Dobrowolski, Acta Phys. Pol. B **46**, 1457 (2015).

[10] H. Arodź, Phys. Rev. E **60**, 1880 (1999).

[11] T. Dobrowolski, Phys. Rev. E **77**, 056608 (2008).

[12] E. Mann, J. Phys. A **30**, 1227 (1997); H. Kleinert and I. Mustapic, J. Math. Phys. **33**, 643 (1992); R. J. Flesch and S. E. Trullinger, *ibid.* **28**, 1619 (1987).

[13] M. J. Rice, Phys. Rev. B **28**, 3587 (1983); J. C. Fernandez, M. J. Goupil, O. Legrand, and G. Reinisch, *ibid.* **34**, 6207 (1986); E. Turlot, D. Esteve, C. Urbina, M. Devoret, R. Grauer, J. C. Fernandez, H. Politano, and G. Reinisch, *ibid.* **42**, 8418 (1990); K. Javidan, J. Phys. A **39**, 10565 (2006).

[14] T. Dobrowolski, Phys. Rev. E **79**, 046601 (2009).

[15] H. Susanto, Phys. Rev. E **73**, 026608 (2006).

[16] K. K. Likharev, O. A. Mukhanov, and V. K. Semenov, RSFQ logic for the Josephson junction technology, in *SQUID '85 -Superconducting Quantum Interference Devices and their Applications*, edited by H. D. Hahlbohm and H. Lobbig (Walter de Gruyter & Co., Berlin, New York, 1985), pp. 1103–1108.

[17] T. Dobrowolski, Eur. Phys. J. B **86**, 346 (2013).

[18] T. Dobrowolski, Curvature effects in 1-D and 2-D Josephson junctions, in *Geometry, Integrability and Quantization*, edited by I. M. Mladenov, A. Ludu, and Akira Yoshioka (Avangard Prima, Sofia, 2014), pp. 127–139.